

Structural and optical properties of sol-gel processed ZnCdMgO nanostructured films as transparent conductor

Praveen Kumar^{1,2}, Amritpal Singh², Dinesh Pathak^{3*}, Ludek Hromadko³, Tomas Wagner³

¹Department of Physics, DAV University, Sarmastpur, Jalandhar 144012, India

²DAV Institute of Engineering and Technology, Kabir Nagar, Jalandhar 144008, India

³Department of General and Inorganic Chemistry, Faculty of Chemical Technology, University of Pardubice, Pardubice, Studentska 573, Pardubice 532 10, Czech Republic

*Corresponding author. E-mail: dinesh.pathak@upce.cz

Received: 27 June 2014, Revised: 22 July 2014 and Accepted: 24 July 2014

ABSTRACT

In the present work, we report the structural and optical properties of sol-gel synthesized $Zn_{0.9}(Cd_{1-x}Mg_x)_{0.1}O$ ($0 \leq x \leq 1.0$) nanostructured films investigated by using the X-ray diffraction, scanning electron microscopy, atomic force microscopy, electrical resistivity, optical absorption and photoluminescence spectroscopic techniques. The X-ray diffraction study has revealed the hexagonal wurtzite crystal structure having favorable c-axis orientation for the increase in Mg concentration. The stress-strain calculation reveals the compressive stresses in Cd rich films whereas Mg rich films experience the tensile stress. Reduction of grain size and surface roughness has been observed with the increase in Mg concentration with more spherical grains. The AFM and SEM micrographs reveal the smooth surface morphology of the synthesized films. The magnesium rich films show high transmission in the visible and NIR region but show decrease in it with the increase in Cd concentration. The band gap increases from 3.19 to 3.40 eV with increase in Mg content. The photoluminescence measurement reveals the decrease in the defects and increase in band gap with the increase in Mg content in the films. The electrical resistivity has been found to be increased from 0.3×10^2 to $169.4 \times 10^2 \Omega\text{-cm}$ with increase in Mg concentration. The present study reports that the compositions $x=0.4$ and $x=0.6$ have the optimized combination of optical transmittance and better electrical resistivity values in this system for their possible applications as transparent conductors. The present results provide important data for TCOs processing with an optimized content of metal dopants for better transparency and conductivity. Copyright © 2014 VBRI press.

Keywords: Thin films; transparent conducting oxides; wide band gap semiconductors; transparency and conductivity.



Praveen Kumar is Ph.D. in Applied Physics (Material Science) and presently working as Assistant Professor of Physics at the DAV University, Jalandhar. In his academic career, he has published 35 research articles in international journal of repute in the field of glassy semiconductors, phase change materials, phase separation effects, nanostructured films, nanocomposites and polymer blends etc.



Dinesh Pathak (Ph.D.) is working as senior researcher at Univerzita Pardubice, Czech Republic. Along with visits to Italy, China, Poland, Spain, Germany, Czech Republic, USA, Canada and Switzerland in regards to his research work and 20+ SCI research papers with reviewing and editorial board member of various scientific journals and events bodies, he was recipient of IUCr award and Rising Star award at AsCA'09 Asian Crystallographic Association and Chinese Crystallography Society at Beijing, China in 2009, alumni of Lindau Council of Noble

prize winners meetings 2012 and visiting scientist at Queen's University Kingston, Canada. His focused research areas are Nanostructured Compound semiconductors, Oxide Nanocomposites and Organic semiconductors/ Organic Inorganic hybrid semiconductor systems.



Tomas Wagner, CSc, University of Pardubice, has been studying amorphous chalcogenides for more than 10 years. His interests cover inorganic chemistry, materials engineering, solid state chemistry, semiconducting materials, preparation and properties of amorphous and glassy chalcogenides, photostructural effects, physical and chemical methods of thin films preparations, thermal analysis, X-ray fluorescence analysis, spectroscopic ellipsometry, micro-optics, and phase change

memories. He is an author or coauthor more than 165 refereed journal papers.

Introduction

Transparent conducting oxides (TCO) with transmittance greater than 80%, while resistivity (ρ) less than 10^{-3} Ω -cm are potential candidates for the various applications in solid state devices such as liquid crystal displays, transducers and solar cells [1]. Zinc oxide is a promising candidate to replace the presently used indium tin oxide as TCO due to its number of properties i.e. large excitation energy (~ 60 meV), wide direct band-gap of 3.37 eV and the ability of band gap engineering with various dopants, makes it a strong contender in this field [2]. Also, ZnO is commercially available with advantages such as comparatively low cost, environment-friendly, non-toxic, high resistance to radiation damage and high thermal and chemical stability. Meanwhile, a lot of research has been done to dope the zinc oxide with different elements i.e. Al, Cd, Mg and In etc. for developing the superior TCO material [3-5]. Different techniques has been used to deposit TCO material films [6-11], while the simplicity along with the variety of process parameters for optimizing the deposition conditions for yielding the highly conducting, more uniformity, and higher transparency for the deposited films.

The use of Cd results in the decrease in the optical gap and electrical resistivity of host ZnO while the use of Mg dopant increases the optical gap as well as the electrical resistivity due to the scattering of charge carriers for above threshold compositions [12-15]. However, we need the materials for TCO applications having smaller values of electrical resistivity and large values optical gap and/or the tailor the band gap for practical applications. Even though, a lot of research has been reported in which ZnO is doped with cadmium or magnesium [3, 4, 6-15], but a very limited literature is available depicting detailed study for Cd, Mg co-doped ZnO films. From last few years doped oxides are attracting researchers for their transparent as well as conducting properties. The present work reports the detailed study of the structure, morphology, optical and electrical properties of sol-gel synthesized Zn (Cd, Mg) O films on the silica glass substrates with an objective to find optimized concentration of metal dopants in ZnO for their applications as transparent conductors.

Experimental

Materials and methods

To prepare $\text{Zn}_{0.9}(\text{Cd}_{1-x}\text{Mg}_x)_{0.1}\text{O}$ thin films, the precursor solution of 0.2 mol/l concentration was prepared by dissolving the zinc acetate dihydrate [$\text{Zn}(\text{CH}_3\text{COO})_2 \cdot 2\text{H}_2\text{O}$, CDH, 99.5% pure] in solvent 2-ethoxyethanol and mixing them with the help of magnetic stirrer with hot plate at 60 °C. While the solution became transparent, ethanolamine [$\text{C}_2\text{H}_7\text{NO}$, Fisher Scientific, 98% pure] was added in 1:1 molar ratio with zinc acetate as sol stabilizer. To deposit $\text{Zn}_{0.9}(\text{Cd}_{1-x}\text{Mg}_x)_{0.1}\text{O}$ ($0 \leq x \leq 1.0$) thin films, appropriate calculated amount of cadmium acetate dihydrate [$\text{Cd}(\text{CH}_3\text{COO})_2 \cdot 2\text{H}_2\text{O}$, SDFCI, 98% pure] and magnesium nitrate hexahydrate (Loba Chemie, 99% pure) was mixed in this solution. The different compositions were made by varying the Cd/Mg concentration for x ($0 \leq x \leq 1.0$). This solution was kept on continuous stirring for an hour at 60

°C and finally the solution became transparent, clear, homogeneous and stable at room temperature. After aging the stable solution up to 24 h for necessary hydrolysis process, the sol was finally spin coated on the well cleaned glass substrates by putting few drops on the center of the substrate and spun at 3000 rpm for 1 min with spin coater. Each deposited layer was preheated at 250 °C on hot plate for 2 minutes. This process was repeated 15 times to obtain films of desired thickness. These thin films were then annealed/ dried in the ambient air conditions at temperature 600 °C in muffle furnace for 1 h.

The crystal phase structure of the films was analyzed by using the X-ray diffractometer (X'Pert PRO, Panalytical, Germany) equipped with a Gionometer PW3050/60 working with Cu K_α radiation (1.54060 Å). The surface morphology of the films was investigated by using atomic force microscope (Solver Pro-M4, SPM, NT-MDT, Russia) operated in contact mode. The surface morphology and elemental concentrations were obtained by scanning electron microscopy/energy-dispersive X-ray spectroscopy (SEM/EDS) (JSM 6610, JEOL Ltd., Akishima, Tokyo, Japan). The optical transmittance spectrum was recorded with the help of UV-Vis spectrophotometer (Evolution 300, Thermo Scientific, USA). The 310 nm line of the xenon arc lamp was used to record the photoluminescence spectra at room temperature using the spectrofluorometer (Lambda 45, Perkin Elmer, USA). Electrical resistivity was measured using two probe method (Scientific Equipments, Roorkee) at room temperature.

Results and discussion

Fig. 1 shows the X-ray diffraction patterns of the $\text{Zn}_{0.9}(\text{Cd}_{1-x}\text{Mg}_x)_{0.1}\text{O}$ thin films. All the diffraction peaks corresponds to the reflection of wurtzite-structured ZnO planes and have a strong (002) peak along with low intensity (100) and (101) peaks. This suggests that all the prepared films have a hexagonal wurtzite structure with preferentially oriented along the c-axis perpendicular to the substrate surface.

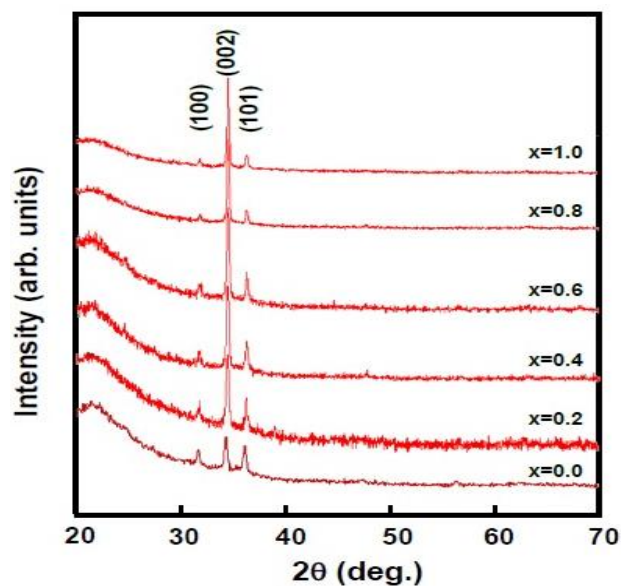


Fig. 1. X-ray diffractograms for the $\text{Zn}_{0.9}(\text{Cd}_{1-x}\text{Mg}_x)_{0.1}\text{O}$ thin films.

However, the intensity of (002) plane is increased with increasing the magnesium content and have maximum intensity for sample $x=1.0$ and minimum for $x=0.0$. No new peaks were found for the like cubic MgO and CdO phases, revealing that the dopants cadmium and/or magnesium does not affects the wurtzite phase of ZnO and hence no phase segregation or secondary phase formation is observed. However with the increase in magnesium content, orientation is more favored along c -axis. The presence of prominent peaks shows that films are polycrystalline in nature. The FWHM varies from 0.0015 for $x=0.2$ to 0.0035 for $x=0.4$ as given in **Table 1**. Thus, the sample with $x=0.2$ has been found of better crystal quality than the other samples. Similar results have also been reported by others workers [3, 19, 20].

Table 1. Summary of various calculated structural parameters viz. peak position (2θ) and fwhm (β) for (002) planes, lattice parameters (a and c), residual stress and crystallite size (D) for $Zn_{0.9}(Cd_{1-x}Mg_x)_{0.1}O$ nanostructure films.

x	Peak (2θ)	b_{002} (rad.)	d (Å)	C (Å)	a (Å)	stress (GPa)	D (nm)
0.0	34.367	0.0029	2.610	5.219	3.013	-0.635	49.70
0.2	34.412	0.0015	2.606	5.212	3.010	-0.331	99.48
0.4	34.486	0.0035	2.601	5.202	3.003	0.156	41.46
0.6	34.526	0.0027	2.598	5.196	3.000	0.414	55.24
0.8	34.467	0.0027	2.602	5.204	3.005	0.027	55.23
1.0	34.498	0.0032	2.600	5.200	3.002	0.231	45.21

For hexagonal wurtzite structure, the lattice parameters, 'a' and 'c' are related to d-spacing and the miller indices h, k and l through the expression [2]:

$$\frac{1}{d^2} = \frac{4}{3} \left(\frac{h^2 + hk + l^2}{a^2} \right) + \frac{l^2}{c^2} \quad (1)$$

where d is the inter planar spacing which is obtained from Bragg's law, and h, k and l are the miller indices denoting the plane. For (002) plane calculated values of 'a' and 'c' lie between $a = 3.000$ to 3.010 Å and $c = 5.196$ to 5.212 Å which agrees with the JCPDS data. This is be clear from the observations that the lattice constant 'c' is increased when Cd^{2+} with higher ionic size (97 pm) replaces Zn^{+2} having a smaller ionic size (74 pm). On the other hand, 'c' shrinks when Zn^{+2} is replaced by Mg^{+2} having smaller ionic size (66 pm) than zinc. The crystallite size of the $Zn_{0.9}(Cd_{1-x}Mg_x)_{0.1}O$ films was calculated using Scherer's formula [21]:

$$D = 0.9 \frac{\lambda}{\beta \cos \theta} \quad (2)$$

where D is the crystallite size, λ is the wavelength of the X-rays used ($=1.54059$ Å), β is the broadening of diffraction line measured at the half of its maximum intensity in radians and θ is the angle of diffraction. The crystallite size along prominent diffraction planes for $Zn_{0.9}(Cd_{1-x}Mg_x)_{0.1}O$ films are given in **Table 1**. The residual stress in the deposited thin films is calculated by using the expression which is valid for hexagonal lattice [22]:

$$stress = \frac{2C_{13}^2 + C_{33}(C_{11} + C_{12})}{2C_{13}} \times \frac{C_{film} - C_{bulk}}{C_{bulk}} \quad (3)$$

which gives,

$$Stress = -233 \frac{(C_{film} - C_{bulk})}{C_{bulk}} GPa \quad (4)$$

where C_{11} , C_{12} , C_{13} , C_{33} are the elastic constants of ZnO film in different directions and have the values 208.8, 119.7, 104.2, 213.8 GPa. C_{bulk} and C_{film} are the lattice constants of standard ZnO powder ($C_{bulk} = 5.205$ nm) and prepared films, respectively. Negative values of stress shows expansion of the structure and positive values of stress show contraction (shrinkage) of the structure and are tabulated in table 1. The observation of compressive stress due to the expansion of the ZnO lattice with the replacement of Zn^{2+} by larger ionic sized Cd^{2+} for the samples with $x=0.0$ and $x=0.2$ samples. While the replacement of Zn with the smaller sized Mg causes the shrinkage of ZnO lattice for favoring the tensile stress. Also, the position of (002) diffraction peak is shifted towards higher angle as the residual stress in the thin films is increased (or the lattice constant 'c' is reduced) with an increase in magnesium concentrations. **Table 1** gives the summary of various calculated structural parameters viz. peak position (2θ) and FWHM value for (002) planes, lattice parameters (a and c), residual stress and crystallite size for $Zn_{0.9}(Cd_{1-x}Mg_x)_{0.1}O$ nanostructure films.

Surface morphology

Fig. 2 shows the 2D and 3D morphological images of the $Zn_{0.9}(Cd_{1-x}Mg_x)_{0.1}O$ films. The results reveal the smooth surface morphology with uniformly sized spherical and some distorted spherical/cubic shaped grains for prepared films.

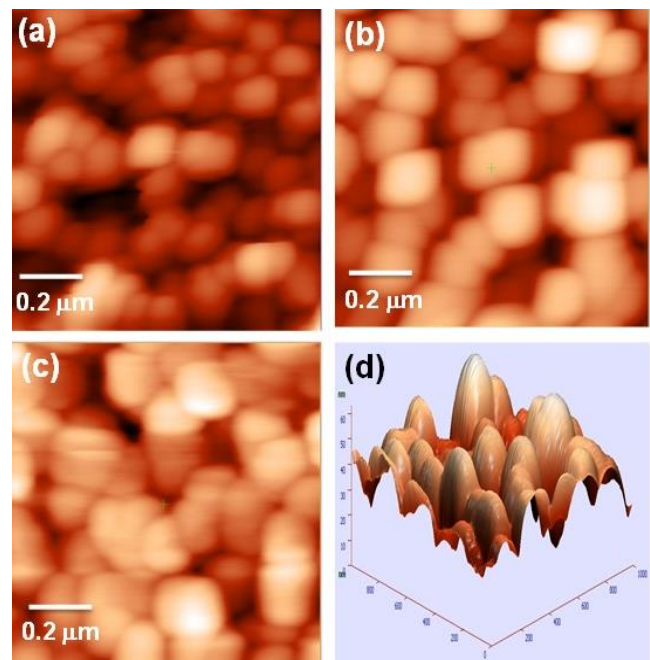


Fig. 2. 2D surface morphological view of (a) $x=0.0$, (b) $x = 0.6$, (c) $x=1.0$ and 3D image for $x=0.6$ in $Zn_{0.9}(Cd_{1-x}Mg_x)_{0.1}O$ thin films.

The calculated values of grain size and rms surface roughness are summarized in **Table 2**. It is observed that the size of the grains decreases from ~50.7- 27.3 nm while the surface roughness decreases approximately from 15.1- 6.3 nm with the increase in magnesium content in the thin films. Similar results have been reported by other workers [23].

Table 2. Summary of various parameters viz. grain size (D_{AFM}), RMS surface roughness (S_q), optical band gap (E_g), PL peaks and electrical resistivity (ρ) of $Zn_{0.9}(Cd_{1-x}Mg_x)_{0.1}O$ thin films.

x	D_{AFM} (nm)	S_q (nm)	E_g (eV)	PL peaks (nm)			ρ ($\times 10^2 \Omega\text{-cm}$)
				I	II	III	
0.0	50.7	15.1	3.18	397	419.5	482.5	0.3
0.2	41.5	12.3	3.21	397	420.0	485.0	2.9
0.4	30.7	09.8	3.25	394	421.5	485.0	17.9
0.6	29.7	09.6	3.28	390	420.5	485.0	41.6
0.8	30.1	08.7	3.30	385	421.5	484.0	124.6
1.0	27.3	06.3	3.40	378	420.0	483.5	169.4

The surface morphology and elemental analysis of the films has also been investigated using SEM-EDS as shown in **Fig. 3**. The SEM images show the smooth surface morphology of the prepared films. The EDS analysis confirmed the presence of Zn, O, Cd and Mg elements in the deposited films.

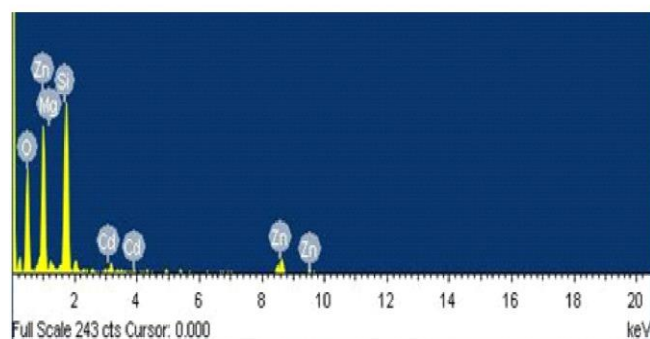
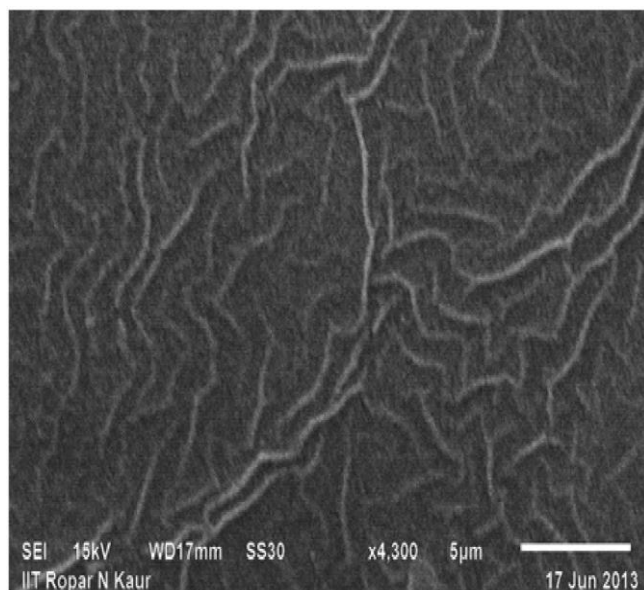


Fig. 3. SEM micrograph and energy dispersive spectra for $Zn_{0.9}(Cd_{1-x}Mg_x)_{0.1}O$ ($x=0.6$) thin films.

Optical properties

Fig. 4 shows the optical transmission spectrum (200–1100 nm) of the films, exhibiting interference fringe patterns with an average transmission more than 86% indicating good optical quality of the deposited films. In the visible and near IR region, the Mg rich films show maximum transmission due to the stable crystal structure, surface morphology as well as the reduction of the optically active defects otherwise the degradation found in the Cd-rich films. These magnesium rich films also block/absorb most of the UV radiations. Similar results were reported by others [4, 11, 24]. It has also been observed that the absorption edge blue shifts with the increase in the Mg concentration in the films indicating band gap broadening [17].

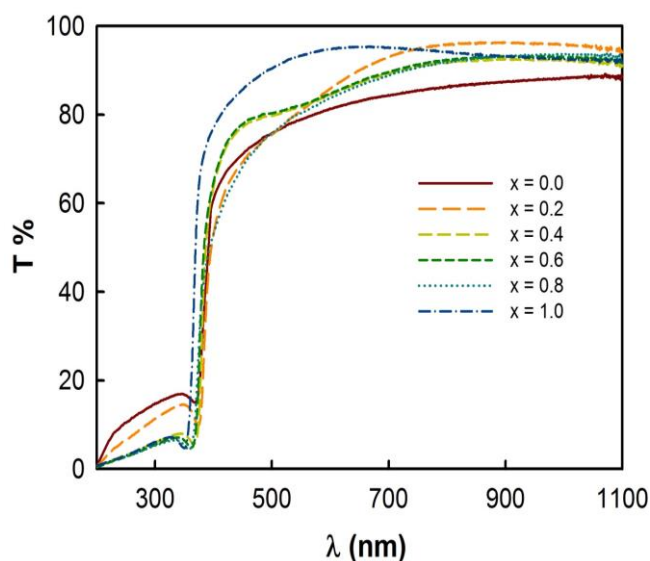


Fig. 4. Optical transmission spectra for $Zn_{0.9}(Cd_{1-x}Mg_x)_{0.1}O$ thin films.

From the transmission spectra, the absorption coefficient (α) is calculated using the relation [25],

$$\alpha(\lambda) = \frac{1}{d} \ln \left(\frac{1}{T} \right) \quad (5)$$

where, d is the film thickness and T is the percentage transmittance of the film. The optical energy gap (E_g) and absorption coefficient α is related by the relation (6), given as;

$$\alpha = \frac{C}{h\nu} \left((h\nu - E_g)^{\frac{1}{2}} \right) \quad (6)$$

which gives

$$((h\nu\alpha)^2) = C(h\nu - E_g) \quad (7)$$

where, E_g is the direct optical band gap energy, $h\nu$ is the incident photon energy, $\beta=1/2$ for direct band gap and C is a constant [26]. The variation of $(h\nu\alpha)^2$ with photon energy ($h\nu$) is shown in **Fig. 5**. The energy gap (E_g) of the samples is evaluated from the intercept of the linear portion of the each curve with $(h\nu)$ on x-axis [18]. It has been found that the values of the optical gap increases from 3.19-3.40

eV with the increase in the Mg content in the samples. Similar results were reported by others [4, 17, 27].

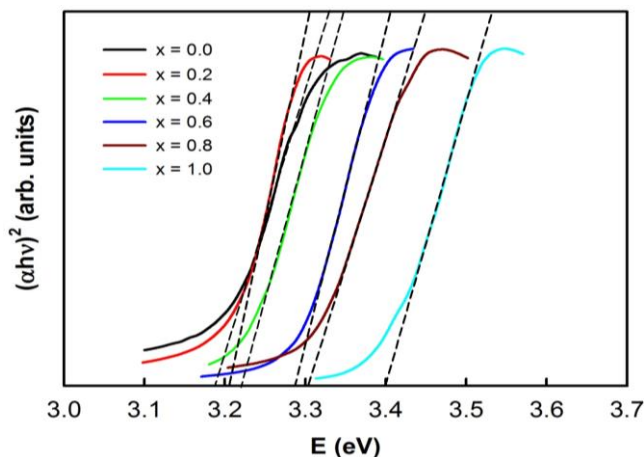


Fig. 5. The variation of $(\alpha h\nu)^2$ versus $h\nu$ for spin coated $\text{Zn}_{0.9}(\text{Cd}_{1-x}\text{Mg}_x)_{0.1}\text{O}$ film samples.

Fig. 6 shows the room temperature photoluminescence spectra of $\text{Zn}_{0.9}(\text{Cd}_{1-x}\text{Mg}_x)_{0.1}\text{O}$ films at an excitation wavelength of 310 nm. A strong dominant UV emission peak has been observed for all the samples related to intrinsic near band edge (NBE) emission at 3.37 eV (380 nm), attributed to the recombination of free excitons through exciton-exciton collision process for the direct band-gap transition of ZnO [28]. However, the peak position of this NBE shifts towards shorter wavelength from 397 nm to 378 nm with the increase in Mg content indicating the band gap broadening [16, 29]. The maximum intensity of this NBE peak in the UV region is for cadmium rich samples attributed to higher density of free excitons. This emission in the near UV region confirms crystal perfection in all the prepared samples.

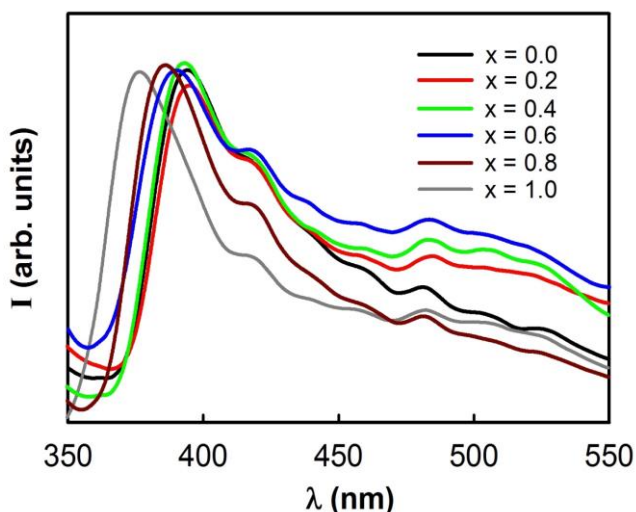


Fig. 6. Room temperature photoluminescence spectra for sol gel synthesized $\text{Zn}_{0.9}(\text{Cd}_{1-x}\text{Mg}_x)_{0.1}\text{O}$ film samples.

Two very low intensity blue emission peaks at 420 nm and 485 nm has been observed for all samples attributed to oxygen related defects (oxygen vacancies or oxygen interstitials) [30]. These defects have been found to decrease with increase in Mg content in the films. A small

intensity peak at 527 nm for $\text{Zn}_{0.9}\text{Cd}_{0.1}\text{O}$ sample, attributed to the deep level defects such as zinc vacancy or oxygen vacancy in ZnO which is being created due to the evaporation of oxygen with the annealing of the sample at 600°C [31]. These donor oxygen vacancies should drag the Fermi level towards the conduction band. Hence the oxygen vacancies created in lattice structure. However, this peak is not broad indicating least porous films structure. Similar results were reported by others workers [15, 19, 28].

Electrical properties

Table 2 summarizes the room temperature electrical resistivity of the $\text{Zn}_{0.9}(\text{Cd}_{1-x}\text{Mg}_x)_{0.1}\text{O}$ films. The resistivity is found to increase with the Mg concentration in the samples and attain highest value of $16.9 \times 10^3 \Omega\text{-cm}$ for $x=1.0$. This large value of the electrical resistivity may be due to the depression of the interstitial metal atom and/or oxygen vacancies of ZnO with Mg doping, which however make these material a p-type or n-type semiconductor [13]. There is also the possibility that a spot of Mg at the grain boundaries may produce electrical barriers, increasing scattering of the carriers, and thus increase the resistivity [14]. On the other hand, low value of electrical resistivity ($0.3 \times 10^2 \Omega\text{-cm}$ for $x=0$) is being observed and hence Cd doping decreases the electrical resistivity [12, 15]. Similar results were reported by others [12-15, 17]. Therefore, the higher transparency along with the low electrical resistivity for the $x=0.4$ and 0.6 samples will be suitable for possible applications as transparent conductors. The optimization of transparency along with conductivity using two metal dopants and low cost sol gel spin coating technique which can be easily scaled to industrial level strengthen novelty of this work.

Conclusion

We have successfully synthesized the $\text{Zn}_{0.9}(\text{Cd}_{1-x}\text{Mg}_x)_{0.1}\text{O}$ ($0 \leq x \leq 1.0$) nanostructured films by low cost sol gel spin coating process. The X-ray diffraction study reveals the hexagonal wurtzite crystal structure with an enhancement in favorable c-axis orientation for Mg rich films. The Cd rich films experience compressive stress whereas Mg rich films experience tensile stress. AFM analysis reveals the formation of highly smooth surface with uniformly distributed spherical or distorted spherical/cubic shaped grains for these films. The SEM-EDS analysis confirmed the stoichiometry of Zn, O, Cd and Mg elements in the synthesized films. The magnesium rich films show high transmission in the visible and NIR region but reduce for Cd-rich films. The band gap increases from 3.19 - 3.40 eV with increase in Mg content. The UV emission peak (NBE) shift towards shorter wavelength from 397-378 nm indicating band gap widening along with the decrease in the optically active defects with the increase in Mg content. The electrical resistivity increases from 0.3×10^2 to $169.4 \times 10^2 \Omega\text{-cm}$ with increase in Mg concentration. These results suggest that the optimized value of the Cd/Mg will be suitable for their application as TCO applications. As the future prospects, we suggest that these systems needs more optimization with various techniques of film synthesis and other metal dopants to find the better conductivity

along with transparency of such systems for technological applications.

Acknowledgements

Dinesh Pathak would like to thank the Ministry of Education, Youth, and Sports of the Czech Republic, Project CZ.1.07/2.3.00/30.0021 'Strengthening of Research and Development Teams at the University of Pardubice', who financially supported him.

Reference

- (a) Advanced Energy Materials, Tiwari, A.; Valyukh, S. (Eds.), Wiley-Scrivener, USA, **2014**. (b) Klein A.; Korber C.; Wachau A.; Sauberlich F.; Gassenbauer Y.; Harvey S.; Proffit D.; Mason T.; *Materials*, **2010**, *3*, 4892.
DOI: [10.3390/ma3114892](https://doi.org/10.3390/ma3114892)
- Muiva C.; Sathiaraj T.; Maabong K.; *Ceramic International*, **2011**, *37*, 555.
DOI: [10.1016/j.ceramint.2010.09.042](https://doi.org/10.1016/j.ceramint.2010.09.042)
- Caglar Y.; Caglar M.; Ilican S.; Ates A.; *Journal of Physics D: Applied Physics*, **2009**, *42*, 065421.
DOI: [10.1088/0022-3727/42/6/065421](https://doi.org/10.1088/0022-3727/42/6/065421)
- Duan L.B.; Zhao X.R.; Liu J.M.; Geng W.C.; Xie H.Y.; Sun H.N.; *Physica Scripta*, **2012**, *85*, 035709.
DOI: [10.1088/0031-8949/85/03/035709](https://doi.org/10.1088/0031-8949/85/03/035709)
- Rokn-Abadi M.; Behdani M.; Arabshahi H.; Hosseini N.; *International Review of Physics*, **2009**, *3*, 219.
- Sadovef S.; Blumstengel S.; Cui J.; Puls J.; Rogaschewski S.; Schafer P.; *Applied Physics Letters*, **2006**, *89*, 201907.
DOI: [10.1063/1.2388250](https://doi.org/10.1063/1.2388250)
- Kumar V.R.; Lethy K.J.; Kumar A.; Krishnan R.; Pillai N.V.; Pillai V.P.M.; Philip R.; *Material Chemistry Physics*, **2010**, *121*, 406.
DOI: [10.1016/j.matchemphys.2010.01.004](https://doi.org/10.1016/j.matchemphys.2010.01.004)
- Ishihara J.; Nakamura A.; Shigemori S.; Aoki T.; Temmyo J.; *Applied Surface Science*, **2005**, *244*, 381.
DOI: [10.1016/j.apsusc.2004.10.094](https://doi.org/10.1016/j.apsusc.2004.10.094)
- Singh T.; Pandya D.K.; Singh R.; *Journal of Alloys and Compounds*, **2011**, *509*, 5095.
DOI: [10.1016/j.jallcom.2011.01.168](https://doi.org/10.1016/j.jallcom.2011.01.168)
- Ma D.W.; Ye Z.Z.; Huang J.Y.; Zhu L.P.; Zhao B.H.; He J.H.; *Material Science and Engineering B*, **2001**, *461*, 250.
DOI: [10.1016/j.mseb.2003.12.007](https://doi.org/10.1016/j.mseb.2003.12.007)
- Ilican S.; Caglar Y.; Caglar M.; *Journal of Optoelectronics and Advanced Materials*, **2008**, *10*, 2578.
- Tabet-Derraz H.; Benramdane N.; Nacer D.; Bouzidi A.; Medles M.; *Solar Energy Materials and Solar Cells*, **2002**, *73*, 249.
DOI: [10.1016/S0927-0248\(01\)00134-9](https://doi.org/10.1016/S0927-0248(01)00134-9)
- Tsay C.; Wang M.; Chiang S.; *Materials Transactions*, **2008**, *49*, 1186.
DOI: [10.2320/matertrans.MER2007334](https://doi.org/10.2320/matertrans.MER2007334)
- Huang K.; Tang Z.; Zhang L.; Yu J.; Lv J.; Liu X.; Liu F.; *Applied Surface Science*, **2012**, *258*, 3710.
DOI: [10.1016/j.apsusc.2011.12.011](https://doi.org/10.1016/j.apsusc.2011.12.011)
- Choi Y.; Lee C.; Cho S.; *Thin Solid Films*, **1996**, *289*, 153.
DOI: [10.1016/S0040-6090\(96\)08923-7](https://doi.org/10.1016/S0040-6090(96)08923-7)
- Singh A.; Kumar D.; Khanna P.K.; Joshi B.C.; Kumar M.; *Applied Surface Science*, **2011**, *258*, 1881.
DOI: [10.1016/j.apsusc.2011.10.096](https://doi.org/10.1016/j.apsusc.2011.10.096)
- Ke Y.; Berry J.; Parilla P.; Zakutayev A.; O'Hayre R.; Ginley D.; *Thin Solid Films*, **2012**, *520*, 3697.
DOI: [10.1016/j.tsf.2011.12.020](https://doi.org/10.1016/j.tsf.2011.12.020)
- Shakti N.; Gupta P.S.; *Applied Physics Research*, **2010**, *2*, 19.
DOI: [10.5539/apr.v2n1p19](https://doi.org/10.5539/apr.v2n1p19)
- Khan Z. R.; Khan M. S.; Zulfequar M.; Khan M.S.; *Material Science and Applications*, **2011**, *2*, 340.
DOI: [10.4236/msa.2011.25044](https://doi.org/10.4236/msa.2011.25044)
- Caglar M.; Caglar Y.; Aksoy S.; Ilican S.; *Applied Surface Science*, **2010**, *256*, 4966.
DOI: [10.1016/j.apsusc.2010.03.010](https://doi.org/10.1016/j.apsusc.2010.03.010)
- (a) Pathak D. ; Bedi R. K. ; Kaur D.; *Materials and Manufacturing Processes* **2010**, *25*,1012
DOI: [10.1080/10426910903367360](https://doi.org/10.1080/10426910903367360)
(b) Pathak D. ; Bedi R. K. ; Kaur D.; *Optoelectronics and Advanced materials – rapid communications*. 05/**2010**; 4,657.
- Wang C.; Xu D.; Xiao X.; Zhang Y.; Zhang D.; *Journal of Material Science*, **2007**, *42*, 9795.
DOI: [10.1007/s10853-007-1992-0](https://doi.org/10.1007/s10853-007-1992-0)
- Ding R.; Xu R.; Gu B.; Shi Z.; Wang H.; Ba L.; Xiao Z.; *Journal of Material Science and Technology*, **2010**, *26*, 601.
- Chun-Jun L.; Hui Z.; Zhi-Qun H.; Chun-Xiu Z.; Dan L.; Yong-Sheng W.; *Chinese Physics Letters*, **2010**, *27*, 097801.
DOI: [10.1088/0256-307X/27/9/097801](https://doi.org/10.1088/0256-307X/27/9/097801)
- Sonawane B.K.; Shelke V.; Bhole M.P.; Patil D.S.; *Journal of Physics Chemistry of Solids*, **2011**, *72*, 1442.
DOI: [10.1016/j.jpccs.2011.08.022](https://doi.org/10.1016/j.jpccs.2011.08.022)
- Park, J.H.; Lim J.B.; Lee B.T.; *Semiconductor Science and Technology*, **2013**, *28*, 065004.
DOI: [10.1088/0268-1242/28/6/065004](https://doi.org/10.1088/0268-1242/28/6/065004)
- Fouzri A.; Boukadhba M.A.; Oumezzine M.; Sallet V.; *Thin Solid Films*, **2012**, *520*, 2582.
DOI: [10.1016/j.tsf.2011.11.027](https://doi.org/10.1016/j.tsf.2011.11.027)
- Gayen N.; Sarkar K.; Hussain S.; Bhar R.; Pal A.; *Indian Journal of Pure and Applied Physics*, **2011**, *49*, 470.
- Vijayalakshmi S.; Venkataraj S.; Jayavel R.; *Journal of Physics D: Applied Physics*, **2008**, *41*, 245403.
DOI: [10.1088/0022-3727/41/24/245403](https://doi.org/10.1088/0022-3727/41/24/245403)
- (a) Singh A.; Kumar P.; *Journal of Optoelectronics and Advanced Materials*, **2014**, *16*, 311. (b) Singh A.; Kumar P.; *International Nano Letters*, **2013**, *3*, 57.
DOI: [10.1186/2228-5326-3-57](https://doi.org/10.1186/2228-5326-3-57)
- Ghods F.; Absalan H.; *Acta Physica Polonica A*, **2010**, *118*, 659.

Advanced Materials Letters

Publish your article in this journal

ADVANCED MATERIALS Letters is an international journal published quarterly. The journal is intended to provide top-quality peer-reviewed research papers in the fascinating field of materials science particularly in the area of structure, synthesis and processing, characterization, advanced-state properties, and applications of materials. All articles are indexed on various databases including DOAJ and are available for download for free. The manuscript management system is completely electronic and has fast and fair peer-review process. The journal includes review articles, research articles, notes, letter to editor and short communications.

